

Anisotropic Self-Diffusion in a Hexagonally Ordered Asymmetric PEP–PDMS Diblock Copolymer Studied by Pulsed Field Gradient NMR

Frank Rittig,* Gerald Fleischer, Jörg Kärger, and Christine M. Papadakis

Fakultät für Physik und Geowissenschaften, Institut für Experimentelle Physik I, Universität Leipzig, Linnéstrasse 5, D-04103 Leipzig, Germany

Kristoffer Almdal

Condensed Matter Physics and Chemistry Department, Risø National Laboratory, P.O. Box 49, DK-4000 Roskilde, Denmark

Petr Štěpánek

Institute of Macromolecular Chemistry, Academy of Sciences of the Czech Republic, CZ-16202 Prague, Czech Republic

Received April 12, 1999; Revised Manuscript Received June 10, 1999

ABSTRACT: The self-diffusion of an asymmetric poly(ethylene-*co*-propylene)-*b*-poly(dimethylsiloxane) diblock copolymer in the hexagonally ordered state is investigated using pulsed field gradient NMR. The order-to-disorder transition (ODT) occurs at $T_{\text{ODT}} = 192\text{ }^{\circ}\text{C}$. A marked nonexponentiality of the echo attenuations is found, and coming from high temperatures, an increase of this nonexponentiality is observed. This is caused by the onset of anisotropic diffusion along the cylinder axes within the hexagonal order whose orientations are randomly (isotropically) distributed in the sample. The echo attenuation curves are fitted by assuming isotropically oriented grains of parallel cylinders with preferentially longitudinal diffusion along the cylinders and slow molecular propagation from cylinder to cylinder, perpendicular to the cylinder axes. The ratio of diffusivities parallel and perpendicular to the cylinders is of the order of 50 at room temperature, decreasing notably with increasing temperatures. The magnitude and activation energy of the diffusivity along the cylinder axes are between those of the corresponding two homopolymers with the same molar masses as the block copolymer.

1. Introduction

Diblock copolymers consist of two chemically different polymer chains joined by a covalent bond. In the melt this class of polymers forms different microphase-separated morphologies below the order-to-disorder transition (ODT) temperature. The state and morphology of diblock copolymers depends on the volume fraction of one block, f , the overall degree of polymerization, N , and the Flory–Huggins interaction parameter, χ , which is inversely proportional to the temperature.¹ Because of the repulsive interaction between both different chain segments, microphase separation into an ordered state takes place for $\chi N > (\chi N)_{\text{ODT}}$. The value of $(\chi N)_{\text{ODT}}$ depends strongly on f . Below $(\chi N)_{\text{ODT}}$, a disordered melt with internal concentration fluctuations is formed. Above this value, a variety of different morphologies occurs, e.g., the lamellar structure, the hexagonal structure consisting of cylinders, and the cubic structure consisting of micelle-like entities, depending on the composition of the diblock copolymer.¹

The relationship between microstructure and dynamics continues to be an attractive area of research. Whereas the structure of diblock copolymers has been thoroughly studied in the past, less is known about their dynamics. Self-diffusion in a microphase-separated diblock copolymer involves different issues: (i) thermodynamic repulsion between A and B segments contacts, which tend to localize the covalent bonds between A- and B-rich domains; (ii) differences in the magnitude

and temperature dependence of the monomeric friction coefficients between blocks, which may depend on composition; and (iii) the mechanism of dynamics (e.g., self-diffusion), which depends on the volume fraction, chain length, and morphology. All these issues arise in considering the anisotropy of diblock copolymer motion in the ordered state: how different are the diffusivities along and through the interface between the different blocks A and B?

Lodge et al. have investigated the tracer and self-diffusion in a lamellar microphase-separated symmetric diblock copolymer by means of macroscopically oriented samples.² In the case of the nonentangled block copolymers, the diffusion was found to be anisotropic: whereas the diffusion along the lamellae (parallel) is not retarded, the diffusion across the interface (perpendicular diffusion) is strongly decreased as a consequence of the thermodynamic repulsion between the two blocks.² In entangled symmetric diblock copolymers both the diffusion along and across the lamellar interfaces is strongly retarded³ because, in addition to the thermodynamic repulsion hindering the perpendicular diffusion, the entanglements prevent the motion of the chains parallel to the interface.

By far less investigated than the dynamics of symmetric diblock copolymers is the dynamics of asymmetric diblock copolymers in the cylindrical ordered state. Lodge et al. have investigated a poly(ethylene-*co*-propylene)-*b*-poly(ethyl ethylene) (PEP–PEE) diblock copolymer showing an order-to-order transition from cylinders to spheres and did not find a discontinuity in the self-diffusion coefficient crossing the order-to-order

* To whom correspondence should be addressed. Fax: +49 341 9732497. E-mail: rittig@physik.uni-leipzig.de.

transition temperature.² Hamersky et al. investigated the self-diffusion in an asymmetric polyethylenoxide-*b*-poly(ethyl ethylene) diblock copolymer using forced Rayleigh scattering (FRS).⁴ In the cylindrical morphology, double-exponential signal decays were found in the isotropically ordered as well as in the macroscopically aligned sample. The nonexponential signal decays have been attributed to diffusion along and across the cylinder axes (in the isotropically ordered sample) and to the diffusion in macroscopically ordered and imperfectly ordered regions (in the macroscopically aligned sample). In this way, anisotropies of diffusion as large as ≈ 80 have been found.

For the cylindrical and the lamellar morphology we expect single-chain diffusion parallel and perpendicular to the interface between A and B blocks. To investigate this anisotropy, two methods can be used: (i) to investigate a macroscopically oriented (i.e., shear-aligned) diblock copolymer sample as a function of rotation angle or (ii) to investigate isotropically oriented samples and to extract the (different) diffusion coefficients from the nonexponentiality of the signal decay. In the present study, we investigate the self-diffusion of an isotropically oriented poly(ethylene-*co*-propylene)-*b*-polydimethylsiloxane (PEP-PDMS) diblock copolymer forming the cylindrical morphology using pulsed field gradient (PFG) NMR. The results are compared to the self-diffusivities of the corresponding homopolymers. We observe a remarkably large anisotropy of motion in the cylindrical phase.

2. Experimental Section

2.1. Sample. The poly(ethylene-*co*-propylene)-*b*-poly(dimethylsiloxane) (PEP-PDMS) diblock copolymer was anionically synthesized^{5,6} and termed PEP-PDMS 21. The molar mass \bar{M}_n is 1.30×10^4 g mol⁻¹ and the polydispersity index $\bar{M}_w/\bar{M}_n = 1.1$. The volume fraction of the minority block, f_{PEP} , is 0.25.⁵ The PEP block is slightly entangled: The entanglement molar mass M_e of PEP is 1500 g mol⁻¹ at 25 °C and 2300 g mol⁻¹ at 140 °C.⁷ The PDMS block is nonentangled ($M_e = 1.3 \times 10^4$ g mol⁻¹). The diblock copolymer is essentially nonentangled because the onset of entanglement effects is not apparent until $M \approx 2.3 \times M_e$.⁸

The ODT temperature is $T_{\text{ODT}} = 192$ °C.⁵ The average diameter of the cylinders was obtained from the position of the first-order Bragg peak in SANS, q^* to, $(\sqrt{(2^5 f_{\text{PEP}} \pi)})/\sqrt{3}/q^* = 9.5$ nm.⁹

An appropriate amount of the copolymer was inserted into an NMR tube, evacuated for 24 h, and sealed under high vacuum.

2.2. PFG NMR. The incoherent intermediate dynamic structure factor, $S_{\text{inc}}(q, t)$, of the diblock copolymer was measured using PFG NMR. A detailed description of this method can be found in refs 10 and 11. The NMR signal was generated by the stimulated-echo rf-pulse sequence: $\pi/2 - \tau - \pi/2 - t' - \pi/2 - \tau - \text{echo}$. The measured spin echo attenuation A/A_0 due to field gradient pulses applied after the first and third $\pi/2$ rf pulse, respectively, is equivalent to the incoherent intermediate scattering function known from neutron scattering.¹²

$$\frac{A}{A_0} = S_{\text{inc}}(q, t) = \int \exp(iqz) P(z, t) dz \quad (1)$$

A and A_0 are the spin echo amplitudes with and without field gradients applied, respectively. $P(z, t)$ is the so-called propagator¹⁰ or the probability density for a displacement of a polymer segment over the distance z within the diffusion time $t = t' + \tau$. $q = |\mathbf{q}| = \gamma \delta g$ is a generalized scattering vector with γ denoting the gyromagnetic ratio of protons, δ the width, and g the magnitude of the gradient pulse. With a Gaussian

propagator (free diffusion), we obtain from eq 1

$$S_{\text{inc}}(q, t) = \exp(-q^2 t D) \quad (2)$$

with

$$\langle z^2 \rangle = 2Dt \quad (3)$$

where D denotes the self-diffusion coefficient and $\langle z^2 \rangle$ the rms displacement of the polymer segments in the z direction during t .

The PFG NMR experiments were carried out with a home-built NMR spectrometer operating at a ¹H-resonance frequency of 400 MHz.^{13,14} In each experiment, τ was chosen to be 3 ms. In each experimental run, δ and t were fixed and g was incremented. The maximum g value was 25 T m⁻¹ and the maximum δ value 1.85 ms. The length scales probed by PFG NMR lie between $1/q_{\text{max}} \approx 80$ nm and a few μm . The diffusion times t were varied between 13 and 603 ms. Equation 2 represents the so-called narrow-pulse approximation $\delta \ll t$ which is fulfilled in our experiments. The experimental error of the temperature is ± 1 K. The upper experimental limit is 200 °C; thus, our investigations are mainly restricted to the ordered phase of PEP-PDMS 21.

2.3. Transverse Nuclear Magnetic Relaxation. Measurements of the transverse nuclear magnetic relaxation times T_2 were carried out at two temperatures using a Bruker AMX 300 spectrometer with a 10-mm selective ¹H probe head using the Carr-Purcell-Meiboom-Gill (CPMG) sequence¹¹ ($\tau = 200$ μs). The data analysis was performed using a program with the regularization technique and self-consistent method.¹⁵

3. Results and Discussion

Typical echo attenuations curves, $S_{\text{inc}}(q, t)$, for different temperatures and observation times are shown in Figure 1. Two main observations are made: The echo attenuations are strongly nonexponential and the echo attenuations lie on a masterplot $S_{\text{inc}}(q, t)$ vs $q^2 t$ over the complete temperature range. This masterplot confirms the validity of eq 3 and the occurrence of unrestricted, ordinary diffusion over the considered time and length scales; diffusion barriers that influence the diffusion in the diblock copolymer on the length scales of our experiment do not exist. Therefore, we have to assign the nonexponentiality of $S_{\text{inc}}(q, t)$ to a distribution of self-diffusion coefficients along the z direction.

We analyzed $S_{\text{inc}}(q, t)$ in terms of the following model for anisotropic diffusion: We assume straight and parallel cylinders ordered in grains (at least over a length of the rms displacements of the chains during t), which are oriented isotropically in the sample ("polycrystalline sample"). In the PFG NMR experiment, the self-diffusion in only one direction (z direction) is measured. The case of diffusion along randomly oriented arrays of elements, each having an axis of cylindrical symmetry, has been calculated previously.^{10,11,16} For the rms displacements along the z axis, in one grain, one obtains

$$\langle z^2 \rangle = 2D_{\text{par}} t \cos^2 \theta \quad (4)$$

where D_{par} is the self-diffusion coefficient for the motion parallel to the cylinder axis and θ denotes the polar angle between the z axis and the cylinder orientation in the grain, i.e., the direction of the displacement; see Figure 2. While $S_{\text{inc}}(q, t)$ for spins residing in a given element will be Gaussian, this is not the case for the powder average. Averaged over all element orientations yields for the spin echo attenuation

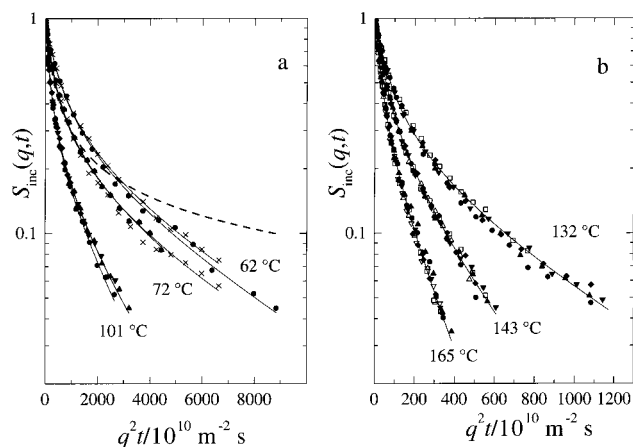


Figure 1. Echo attenuations $S_{\text{inc}}(q, t)$ vs $q^2 t$ in a semilogarithmic representation at the temperatures indicated and at $t = 23$ ms (∇), 33 ms (\triangle), 53 ms (\square), 103 ms (\blacklozenge), 203 ms (\blacktriangledown), 303 ms (\triangle), 453 ms (\times), and 603 ms (\bullet). The full lines are fits to eq 7. The dashed line in (a) shows a fit of eq 7 with $D_{\text{perp}} = 0$ for 62 °C.

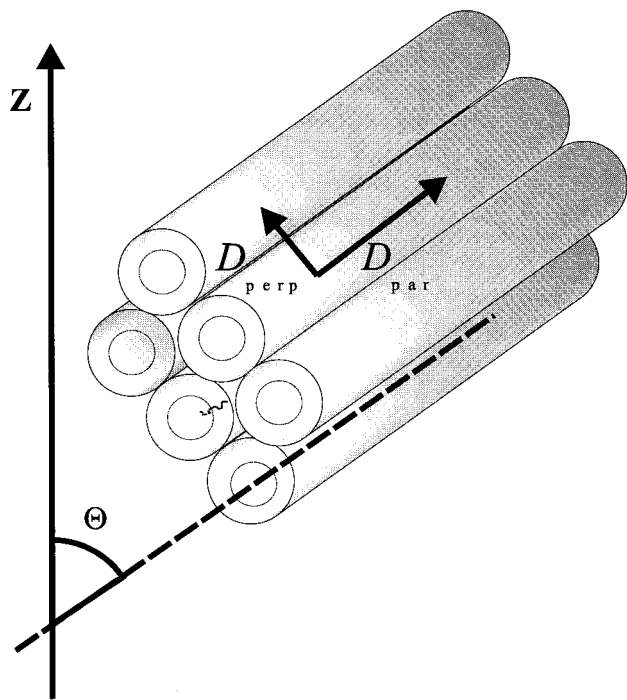


Figure 2. Schematic illustration of a grain from the ordered diblock copolymer and the diffusion parallel and perpendicular to the axes of the cylinders. θ is the angle between the orientation of the cylinders and the laboratory axis z (direction of the pulsed field gradients) in which the self-diffusivity is measured.

$$S_{\text{inc}}(q, t) = \int_0^\pi \exp(-q^2 t D_{\text{par}} \cos^2 \theta) \sin \theta d\theta \quad (5)$$

The result is a strongly nonexponential echo attenuation which is indicated as the dashed curve in Figure 1a. The measured echo attenuations, however, are less nonexponential than those described by this model. We assign this deviation to slow chain diffusion perpendicular to the cylinder axes, i.e., to $D_{\text{perp}} > 0$ (see Figure 2).

If diffusion perpendicular to the cylinder axis is permitted, the rms displacement is given by

$$\langle z^2 \rangle = 2t(D_{\text{par}} \cos^2 \theta + D_{\text{perp}} \sin^2 \theta) \quad (6)$$

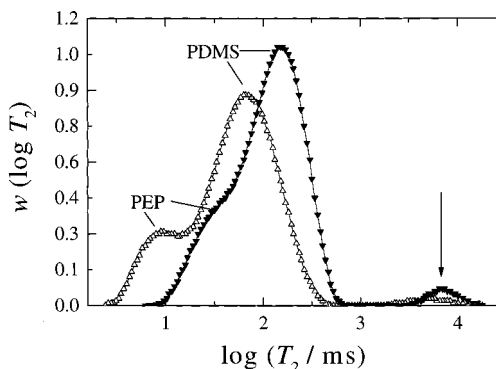


Figure 3. Distribution $w(\log T_2)$ of transverse nuclear magnetic relaxation times T_2 in the diblock copolymer at $T = 22$ °C (\triangle) and 50 °C (\blacktriangledown). The arrow, the peak of the free chains in the hexagonal state.

Now, averaging over all element orientations leads to

$$S_{\text{inc}}(q, t) = \int_0^\pi \exp[-q^2 t (D_{\text{par}} \cos^2 \theta + D_{\text{perp}} \sin^2 \theta)] \sin \theta d\theta \quad (7)$$

Fitting eq 7 to the data yields two parameters: the diffusion coefficient parallel to the cylinder axis D_{par} and the (inverse) anisotropy of motion, $D_{\text{perp}}/D_{\text{par}}$. The integration in eq 7 was carried out numerically and the expression obtained was fitted to the experimental data. This type of analysis has also been successfully when applied to the study of diffusion in the channels of mesoporous adsorbents of type MCM 41.¹⁷ These fits are shown as full lines in Figure 1. However, slight deviations from the fits are observed in the initial part of $q^2 t \rightarrow 0$ of the echo attenuations which we attribute to the existence of “free chains” in the matrix between the cylinders. An additional indication of the existence of these free chains is shown in Figure 3, where the distributions of T_2 relaxation times for two temperatures are presented. Besides the peaks related to the relaxation of the two blocks of the diblock copolymer in the ordered state (the main peaks at $T_2 < 10^3$ ms), a weak peak at large relaxation times is observed which we attribute to free chains in the diblock copolymer melt. The amplitude of this peak increases with temperature. We are not able to separate the diffusion coefficient of the free chains from the diffusion coefficient of the chains forming the cylinder and diffusing parallel to the cylinder axis, D_{par} , i.e., to decompose the $S_{\text{inc}}(q, t)$ in one part of the free chains and one part of the chains confined to the cylinders. Note that the two blocks of the chains (PEP and PDMS) have different T_2 values: The short T_2 can be attributed to the PEP block (in the cylindrical core) and the peak with the intermediate T_2 value to the PDMS (matrix).

Let us now return to the deviations from our model. For temperatures below ~ 132 °C the echo attenuations slightly split for different times, t . The observed non-exponentiality becomes weaker with increasing t . We attribute this effect to diffusion along curved paths, which is observed when the experimental time scale is sufficiently long. The motion is still confined to one-dimensional elements but now along a curvilinear path. If the cylinders are bent, motion along cylinders which are initially oriented perpendicular to the laboratory z axis contribute to $\langle z^2 \rangle$. Therefore, the echo attenuations become more and more exponential with increasing diffusion time t as shown in Figure 1a.

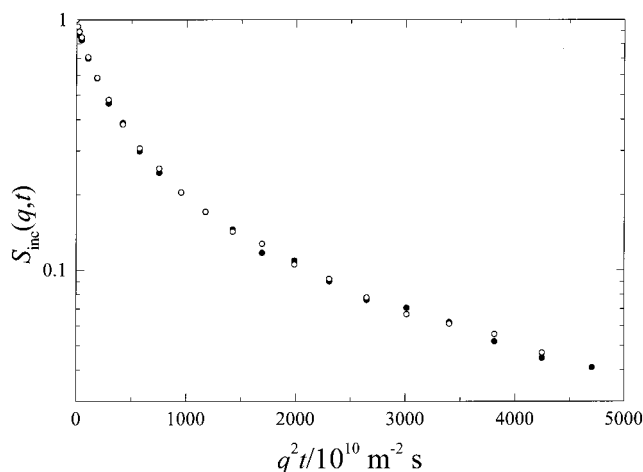


Figure 4. Echo attenuations $S_{\text{inc}}(q, t)$ vs $q^2 t$ in a semilogarithmic representation at the temperature $T = 80^\circ\text{C}$ for $t = 603$ ms with different repetition times (2 s, open; 10 s, filled symbols).

One might argue that because of the existence of two different states of diblock copolymers (free chains and cylinder-forming chains), different spin-lattice relaxation times T_1 are present and, therefore, an apparent t dependence of the echo attenuation should be observed. This is not the case because if different longitudinal nuclear magnetic relaxation times exist due to the presence of diblock copolymer chains with different mobility, they are averaged out because of spin diffusion.¹⁸ We have carried out an experiment to prove this hypothesis: Measurements at 80°C with different repetition times (2 and 10 s) and therefore different time intervals for T_1 relaxation gave nearly identical echo attenuation curves for all observation times t . An example is shown in Figure 4. We conclude from the results of these experiments that different T_1 values cannot be the reason for the time dependence of the echo attenuations. The time dependence of the curves below $\sim 132^\circ\text{C}$ can thus only be explained by slightly bent cylinders.

We now discuss the anisotropy of diffusion, $D_{\text{par}}/D_{\text{perp}}$. From the fits of the expression given in eq 7 values of the diffusivities parallel (D_{par}) and perpendicular (D_{perp}) to the cylinders were extracted. The mobility across the cylinders increases with temperature from $D_{\text{perp}} \approx D_{\text{par}}/60$ at 60°C up to $D_{\text{perp}} \approx D_{\text{par}}/5$ at 195°C . The anisotropy is remarkably high and the straight length of the cylinders seems to be in the order of micrometers. In a PEP-PDMS diblock copolymer forming a lamellar structure, a parallel order of lamellae over only ≈ 60 nm was found.¹⁹ The values determined were similar to the anisotropy previously reported for the cylindrical morphology by Hamersky et al.⁴ The FRS method used by Hamersky et al. works analogously to PFG NMR⁴ in that it monitors the single-particle correlation function of the diffusing species in one dimension in space. Hamersky et al. analyzed the signal decay in the isotropically oriented sample in terms of a sum of two exponentials which they attributed to diffusion parallel and perpendicular to the cylindrical axes. But each chain has to change many times between different cylinders during the measuring time; therefore, only an averaged self-diffusion coefficient should be measured. The nonexponentiality of the signal decay should arise from the distribution of cylinder axes (an increase of nonexponentiality with decreasing diffusion length or

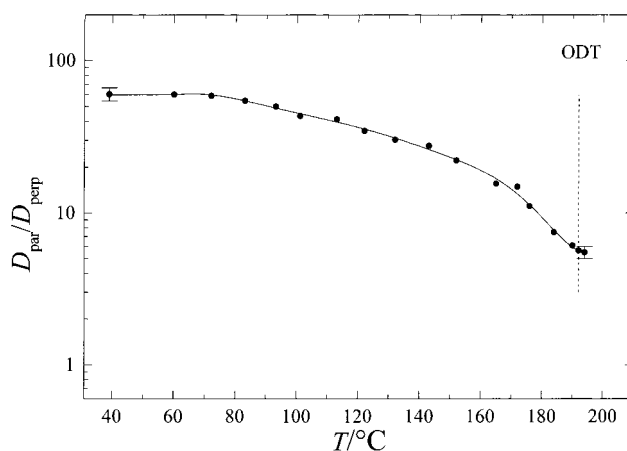


Figure 5. Dependence of the diffusion anisotropy $D_{\text{par}}/D_{\text{perp}}$ on temperature. The full line is a guide to the eye.

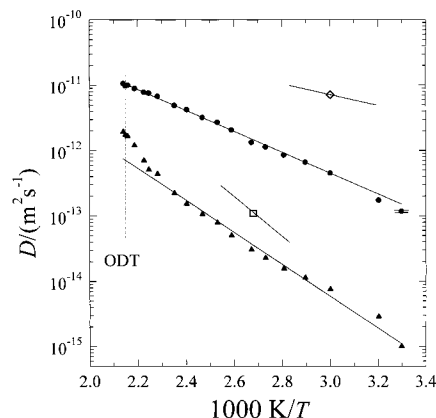


Figure 6. Arrhenius plot of the self-diffusivities D_{par} (●) and D_{perp} (▲) of the diblock copolymer. The self-diffusivities of a PEP homopolymer of $M = 12\,500$ g mol⁻¹ from ref 21 (□) and a PDMS homopolymer of $M = 12\,500$ g mol⁻¹ from ref 20 (○) and their temperature dependences are also depicted.

grating spaces can be seen in Figure 6 of ref 4). The same argument should play a role in diffusion in the shear-aligned sample: during a typical measuring time of 100 s the chains have to move a distance between perfectly and imperfectly aligned regions. Nevertheless, the conclusions drawn from the experiments of Hamersky et al. are very convincing, but additional experiments are desirable.

Our experimentally found anisotropy decreases monotonously with increasing temperature (Figure 5). We find that, even at the ODT temperature, $S_{\text{inc}}(q, t)$ is nonexponential. To explain this, we have to consider a distribution of diffusion coefficients due to the polydispersity in molar mass affecting also the diffusivities both parallel and perpendicular to the cylinder axis. For this strongly asymmetric sample, the thermodynamic repulsion is rather high at T_{ODT} ($\chi N > 33$); i.e., concentration fluctuations are present in the disordered state right above T_{ODT} . We conclude that above T_{ODT} the nonexponentiality is due to fluctuations in composition as well as to polydispersity. As we are not able to separate the anisotropy from the polydispersity at the highest temperatures, the anisotropy obtained by fitting with eq 7 is too high near the ODT.

We now turn to an examination of the temperature dependence of the diffusion coefficient along the cylinder axis, D_{par} (Figure 6). For comparison, the self-diffusivities of PEP and PDMS homopolymers having the same

molar mass as the diblock copolymer are shown as well. The observed temperature dependence follows an Arrhenius law with the activation energy of $E_A = (31 \pm 1)$ kJ mol⁻¹, which is between that of PDMS (16 kJ/mol²⁰) and PEP (58 kJ/mol²¹) diffusion. This is not surprising since the diffusion of a chain moving along the cylinders is subjected to the monomeric friction coefficients of either blocks, PDMS and PEP.

In Figure 6, the diffusion coefficient perpendicular to the cylinder axis D_{perp} is shown as well. For temperatures below 165 °C, $\log D_{\text{perp}}$ depends linearly on the inverse temperature. The motion perpendicular to the cylinder axis is determined by the monomeric friction of PEP and PDMS as well as by the thermodynamic repulsion between the different blocks. If an individual chain propagates in a way that its PEP block moves from the core of one cylinder to another, this block must pass through a matrix consisting of PDMS block copolymer chains. The diblock copolymer thus has to pass an energy barrier, corresponding to the repulsive interaction between PEP segments and the PDMS matrix. For thermal activation over this barrier, D_{perp} is given by

$$D_{\text{perp}} \propto D_0 \exp(-\alpha f_{\chi} N) \quad (8)$$

where D_0 is the self-diffusion coefficient of the copolymer chain in a (hypothetical) homogeneous state at the temperature of interest and depends on the mechanisms of motion in the absence of the thermodynamic interaction. α is a constant of order 1. For the magnitude and temperature dependence of the diffusion coefficient D_0 in the hypothetical homogeneous state, we have taken the self-diffusion coefficient of a PEP-PDMS diblock copolymer having nearly the same degree of polymerization and a volume fraction of the minority block $f_{\text{PEP}} = 0.22$ (which is close to 0.25 of the sample studied here) which was investigated by us in a previous work.²² The magnitude and temperature dependence of the diffusion coefficient found in the disordered state should be close to $D_0(T)$ for the actual sample. For the Flory-Huggins parameter different values have been proposed. Schwahn et al.²³ estimated the mean field equivalent χ parameter for a symmetric PEP-PDMS to be $\chi(T) = 82 \text{ K}/T - 2 \times 10^{-2}$. Whereas Vigild⁵ estimated the χ parameter to be $\chi(T) = 64 \text{ K}/T - 3 \times 10^{-2}$. By combining eq 8 with this relation and fitting to the data of D_{perp} , we obtain $\alpha = 0.34 \dots 0.46$. These values are comparable to what was found before: $\alpha = 0.5$ in a lamellar PEP-PEE system³ and $\alpha = 1.2$ in a spherical PVP-PS diblock copolymer.²⁴

For temperatures above 165 °C, D_{perp} increases more strongly than what was predicted from eq 8, and we find $\alpha = 0.5$. We explain this behavior by assuming that the model of thermal activation to cross the interface (eq 8) fails because of an increasing number of defects in the cylindrical morphology. Also, for temperatures not far below the order-to-disorder transition, the composition profile is not sharp, promoting motion across such interfaces.

4. Summary

The self-diffusion of an asymmetric PEP-PDMS diblock copolymer below the order-to-disorder transition temperature ($T_{\text{ODT}} = 192$ °C) has been investigated by means of pulsed field gradient NMR. In the ordered state, the diblock copolymer forms a cylindrical morphology.

We have found a strong nonexponentiality of the echo attenuations which reflects the anisotropy of motion in the sample. For describing the nonexponentiality of the echo attenuations, we have used a model assuming diffusion along the cylinders and (slow) perpendicular propagation from cylinder to cylinder in a sample of isotropically oriented grains consisting of straight parallel cylinders. The resulting values for the diffusion coefficients along (D_{par}) and across (D_{perp}) the cylinder axes differ by factors between 60 at $T = 60$ °C and 5 at $T = 190$ °C. The results are in good agreement with the previously reported anisotropy by Hamersky et al.⁴ and Ehlich et al.²⁵ Below 132 °C we found that the echo attenuations slightly depend on the observation time. We speculate that the deviations are due to bent cylinders.

An activation energy of 31 ± 1 kJ mol⁻¹ is found for the motion along the cylinder axis which is between that of PDMS and PEP diffusion, as expected. Close to the ODT temperature still a marked nonexponentiality of the echo attenuation is found which is caused by anisotropy of motion, concentration fluctuations, and polydispersity of chain length.

Acknowledgment. G.F., J.K., and F.R. acknowledge financial support from the Deutsche Forschungsgemeinschaft (SFB 294). P.Š. thanks the Grant Agency of the Czech Republic (Grant No. 203/99/0573). The authors thank Dr. A. Werner, Department of Medical Physics and Biophysics, University of Leipzig, for the T_2 measurements.

References and Notes

- (1) Bates, F. S.; Fredrickson, G. H. *Annu. Rev. Phys. Chem.* **1990**, *41*, 525. Bates, F. S. *Science* **1991**, *251*, 898. Fredrickson, G. H.; Bates, F. S. *Annu. Rev. Mater. Sci.* **1996**, *26*, 501.
- (2) Lodge, T. P.; Hamersky, M. W.; Milhaupt, J. M.; Kannan, R. M.; Dalvi, M. C.; Eastman, C. E. *Macromol. Symp.* **1997**, *121*, 219.
- (3) Lodge, T. P.; Dalvi, M. C. *Phys. Rev. Lett.* **1995**, *75*, 657.
- (4) Hamersky, M. W.; Hillmyer, M. A.; Tirrell, M.; Bates, F. S.; Lodge, T. P.; von Meerwall, E. D. *Macromolecules* **1998**, *31*, 5363.
- (5) Vigild, M. E. Ph.D. Thesis, Risø National Laboratory, Roskilde, Denmark, 1997.
- (6) Ndoni, S.; Papadakis, C. M.; Bates, F. S.; Almdal, K. *Rev. Sci. Instrum.* **1995**, *66*, 1090.
- (7) Fetters, L. J.; Lohse, D. J.; Richter, D.; Witten, T. A.; Zirkel, A. *Macromolecules* **1994**, *27*, 4639.
- (8) Ferry, J. D. *Viscoelastic Properties of Polymers*, 3rd ed.; Wiley: New York, 1980.
- (9) Papadakis, C. M.; Almdal, K.; Mortensen, K.; Rittig, F.; Fleischer, G.; Štěpánek, P., in preparation.
- (10) Kärger, J.; Pfeifer, H.; Heink, W. *Adv. Magn. Reson.* **1988**, *12*, 1.
- (11) Callaghan, P. T. *Principles of Nuclear Magnetic Resonance*, 1st ed.; Clarendon Press: Oxford, 1993.
- (12) Fleischer, G.; Fujara, F. *NMR: Basic Princ. Prog.* **1994**, *30*, 161.
- (13) Heink, W.; Kärger, J.; Seiffert, G.; Fleischer, G.; Rauchfuss, J. J. *Magn. Res. A* **1995**, *114*, 101.
- (14) Kärger, J.; Bär, N.-K.; Heink, W.; Pfeifer, H.; Seiffert, G. *Z. Naturforsch.* **1995**, *50A*, 186.
- (15) Schäfer, H.; Albrecht, R.; Richert, R. *Chem. Phys.* **1990**, *182*, 53. Schäfer, H. Ph.D. Thesis, Universität Leipzig, Leipzig, Germany, 1994.
- (16) Callaghan, P. T.; Jolley, K. W.; Lelievre, J. *Biophys. J.* **1979**, *28*, 133.
- (17) Kärger, J.; Schäfer, H. In *Fundamentals of Adsorption*; Munier, F., Ed.; Elsevier: Paris, 1998.
- (18) Schmidt-Rohr, K.; Spiess, H. W. *Multidimensional Solid-State NMR and Polymers*; Academic Press, Harcourt Brace & Company: London, 1994.
- (19) Fleischer, G.; Rittig, F.; Štěpánek, P.; Almdal, K.; Papadakis, C. M. *Macromolecules* **1999**, *32*, 1956.
- (20) Appel, M.; Fleischer, G. *Macromolecules* **1993**, *26*, 5520.

- (21) Pearson, D. S.; Fetters, L. J.; Graessley, W. W.; Ver Strate, G.; von Meerwall, E. *Macromolecules* **1994**, *27*, 711. Shull, K. R.; Kramer, E. J.; Bates, S. F.; Rosedale, J. A. *Macromolecules* **1991**, *24*, 1383.
- (22) Fleischer, G.; Rittig, F.; Kärger, J.; Štěpánek, P.; Papadakis, C. M.; Mortensen, K.; Almdal, K. *J. Chem. Phys.* **1999**, *111*, 2789.

- (23) Schwahn, D.; Frielinghaus, H.; Mortensen, K.; Almdal, K. *Phys. Rev. Lett.* **1996**, *77*, 3153.
- (24) Yokoyama, H.; Kramer, E. J. *Macromolecules* **1998**, *31*, 7871.
- (25) Ehlich, D.; Takenaka, M.; Hashimoto, T. *Macromolecules* **1993**, *26*, 492.

MA990548U